Effect of functionalization and concentration of carbon nanotubes on mechanical, wear and fatigue behaviours of polyoxymethylene/carbon nanotube nanocomposites

BHANU K GORIPARTHI[1], P N E NAVEEN[2], H RAVI SANKAR[3] and SOMNATH GHOSH[4],*

[1]Department of Mechanical Engineering, IIIT RK Valley, RGUKT-AP, RK Valley 516330, India
[2]Department of Mechanical Engineering, Godavari Institute of Engineering and Technology, Rajahmundry 533201, India
[3]Department of Mechanical Engineering, Central Research Laboratory (CRL), GITAM University, Visakhapatnam 530045, India
[4]Faculty of Chemistry, Indian Institute of Petroleum and Energy (IIPE), Visakhapatnam 530003, India
*Author for correspondence (ghoshmnth@gmail.com)

Abstract. The main focus of this work is to improve the mechanical, wear and fatigue behaviours of polyoxymethylene (POM) by reinforcing with carbon nanotubes (CNTs). To improve compatibility between CNTs and POM, the surface of the CNTs was modified by various methods of functionalization like carboxylation, silanation, carbonylation and amination. The functionalized CNTs were characterized by Fourier transform infrared spectroscopy to confirm the different functional groups attached to the surface. POM/CNT nanocomposites were developed with functionalized CNTs in different concentrations varying from 0.25 to 2 wt%. Nanocomposites with 1 wt% of silanated CNTs resulted in maximum improvement of tensile, flexural and impact properties. Furthermore, experimental results on fatigue and dry sliding wear tests revealed that the fatigue strength, specific wear rate and friction coefficient are sensitive to functionalization and concentration of CNTs.

Keywords. Carbon nanotubes; silanation; carboxylation; amination; carbonylation; wear; fatigue.

1. Introduction

Polymer gears are extensively used in food processing, automobile, aerospace and biomedical industries due to their noiseless performance, oil-less conditions and low cost [1]. Polyoxymethylene (POM) is one among the widely accepted polymer gear material due to its unique properties, such as abrasion resistance, low friction coefficient, fatigue resistance, dimensional stability, etc. However, stiffness, fatigue strength and wear resistance of polymer gear material have a detrimental effect on life and load bearing capacity of the gears [2]. To widen the range of applicability of the POM gears, these properties need to be enhanced. Improved stiffness and fatigue strength decreases the internal heat generation due to hysteresis effect and the enhanced wear resistance decreases surface temperature generated at the mating gear tooth, which in turn results in increased load bearing capacity and life of the gear. Through the years, many researchers have attempted to improve the life and load bearing capacity of polymer gears by reinforcing the gear materials with fibrous materials (glass fibre, carbon fibre, etc.) and by blending with lubricating additives such as polytetrafluoroethylene (PTFE), MoS_2, etc. A recent trend in polymer research is to explore the synergistic effect of nanoreinforcements in improving the various properties of polymers. Among

various nanoreinforcements, carbon nanotubes (CNTs) seem to be a promising alternative for reinforcing polymers due to its excellent mechanical properties, low density, high surface area and high aspect ratio [3–5]. However, the properties of the CNT-based nanocomposites strongly depend on the dispersion state of CNTs in the polymer matrix and on the interfacial interaction between CNTs and the polymer matrix [6]. Though, a large quantum of data is available on the polymer/CNT composites with matrices like epoxy, polyamide, polyimide, etc., very little information is available on POM/CNT composites [7–11] due to poor compatibility of POM with other materials.

Dispersion is a challenging issue that needs to be addressed for achieving better mechanical properties of CNT/polymer nanocomposites. Uniform dispersion of CNTs in the polymer matrix will result in increase of the surface area available for bonding with matrix and also prevents the agglomerations which act as stress concentrators. However, CNTs are difficult to disperse in polymer matrices as they tend to agglomerate and entangle due to their high aspect ratio and van der Walls interactions [6]. Apart from dispersion, a strong interfacial bonding between CNTs and the polymer matrix is highly desirable as the mechanical properties of the nanocomposites stem from the load transfer capability between the matrix and the reinforcement. The efficiency of load transfer

depends on interfacial bonding between the CNTs and the polymer matrix. But the non-reactive nature of the CNTs will cause weak interfacial adhesion with the matrix which in turn impedes the efficient load transfer between matrix and reinforcement [12]. Hence, to overcome these two key challenges, the surface of the CNTs has been modified by various chemical functionalization methods. However, very few studies have been reported on functionalized CNT reinforced POM composites. Moreover, the effect of various types of functionalization of CNTs on wear and fatigue behaviour of CNT reinforced composites is seldom reported.

Zhao and Ye [9] enhanced the dispersion and affinity of multi-walled carbon nanotubes (MWCNTs) with POM by functionalizing nanotubes with PEG-substituted amine. Functionalized CNT/POM composites exhibited notable improvement in mechanical and thermal properties. Hong *et al* [13] dispersed pristine and carboxyl (–COOH) functionalized MWCNTs into epoxy resin using a three roll mill. Carboxylic functionalization has resulted in significant improvement of the modulus as compared to pristine CNTs. Zhao *et al* [14] incorporated carboxylated and pristine CNTs into PA6 via *in situ* polymerization. At 0.5 wt% of CNT concentration, tensile strength was increased by 7.6 and 8.2%, respectively, for pristine CNT/PA6 composites and carboxylated CNT/PA6 composites as compared to neat PA6. Kim *et al* [15] studied the effect of oxidation and amine functionalization on the fracture toughness of epoxy composites. Amine functionalized composites have exhibited higher fracture toughness as compared to oxidized and pristine CNT composites. Grafting of silane coupling agent on to CNT surface has improved the dispersion along with mechanical and thermal properties as compared to pristine CNT nanocomposites [16]. Liu *et al* [17] prepared PA6/acid-modified CNTs by using melt compounding. A uniform dispersion and strong interfacial adhesion of acid-treated CNTs with PA6 were reported. Strength and modulus were found to be significantly improved by ∼124 and 115%, respectively, with incorporation of 1 wt% acid-treated CNTs. Meng *et al* [18] studied the effect of acid and diamine modification of CNTs on mechanical properties of polyamide6/CNT nanocomposites. They found a significant improvement in Young's modulus, yield strength and storage modulus with the incorporation of diamine-modified CNTs in PA6. Yuen *et al* [19] showed that amine-modified CNTs had better dispersion and strong interfacial adhesion with polyimide matrix as compared to raw CNTs. Cui *et al* [20] investigated the effect of grafting carboxylation and amino groups on the CNTs on the wear behaviour of CNT/epoxy composites. Of all the weight fractions considered, composites with amino functionalized CNTs exhibited the lowest specific wear rate and friction coefficient as compared to composites with pristine and acid-treated CNT. Sulong *et al* [21] observed a better tribological behaviour for composites with functionalized CNTs as compared to composites with the as-produced CNTs. Lee *et al* [22] fabricated ultra-high molecular weight polyethylene (UHMWPE)/CNT

composites with oxidized and silanized CNTs. The effect of functionalization of CNTs on wear behaviour is investigated through wear tests. The silanized UHMWPE/CNT composites exhibited lower specific wear rate and coefficient of friction as compared to UHMWPE/oxidized CNT and UHMWPE/raw CNT composites. Zhang *et al* [23] observed that the fatigue crack growth can be reduced significantly by improving the dispersion of CNTs. Reviewing the literature, it can be understood that the surface modification of CNTs has often led to better dispersion of CNTs in the polymer matrix and improved the interfacial bonding between matrix and CNTs. This in turn has resulted in the enhancement of mechanical properties of CNTs based polymer nanocomposites. However, the effect of various methods of functionalization on CNT/POM composites is seldom reported. Nevertheless, for a given polymer, identification of effective surface modification is a key challenge and hence investigating the effect of various methods of functionalization of CNTs on the same polymer matrix is very important. Hence, an attempt is made to identify effective CNT functionalization so as to improve the mechanical propeties, fatigue strength and wear resistance of POM, with an ultimate objective to enhance the life and load bearing capacity of POM gears. In the present work, POM/CNT composites were developed by melt compounding using a twin screw extruder. To achieve better dispersion of CNTs in the POM and improve the interfacial bonding with the POM matrix, surface of the CNTs was modified by various methods like carboxylation, silanation, carbonylation and amination. Spectral analysis is carried out to ensure the surface modifications of CNTs. Tensile, flexural, impact, wear and fatigue behaviours of the developed nanocomposites were investigated to assess the influence of various methods of functionalization.

2. Experimental

2.1 *Materials*

POM copolymer (also popularly known as polyacetal), the most commonly used engineering thermoplastic was used as base material in this work. A granular POM copolymer with a trade name of Kocetal K 700, supplied by Kolon Engineering Plastics, USA, was utilized in this study. MWCNTs, supplied by Sky Spring Nano Inc., USA, with an outer diameter of 20–30 nm and length of 10–30 μm were used in this work for reinforcing POM. CNTs are synthesized from natural gas via the catalytic chemical vapour deposition technique. For functionalization of CNTs, hydrochloric acid, sulphuric acid, nitric acid, ethanol, distilled water, thionyl chloride, acetone and ethylene diamine (EDA) were purchased from Lotus Enterprises Ltd., India. Silane coupling agent 3-aminopropyltrimethoxy silane (ATPS) was procured from TCI Chemicals, Japan.

2.2 *Methods*

2.2a *Functionalization of MWCNTs*:

To obtain a uniform dispersion of CNT in the matrix and to achieve better compatibility of CNT with the matrix, surface modifications of CNT were done by using various methods like carboxylation, silanation, carbonylation and amination. The procedure carried out for these surface modifications is detailed in the following sections.

2.2b *Purification of MWCNTs*:

Initially, CNTs were purified in two stages to remove the amorphous carbon and other impurities. The as-received CNTs were calcined at 500°C for 45 min to remove volatile gases and other impurities. After calcinations, calcined CNTs were dispersed in a mixture of concentrated HCl and distilled water (1:1 by volume) and stirred for 5 h using a magnetic stirrer. Then, the suspension was allowed to settle for 24 h and after removing these impurities, the suspension was washed thoroughly with distilled water and vacuum filtered using 0.22 μm PTFE membrane until the pH value of 7 was attained. The filtered solid was dried in a vacuum oven and is referred to as R-CNTs hereafter.

2.2c *Carboxylation*:

R-CNTs were oxidized with a mixture of concentrated sulphuric acid and nitric acid (3:1 by volume). For this purpose, R-CNTs were refluxed in a 3:1 mixture of H_2SO_4:HNO_3 at 90°C for 8 h. After refluxing for 8 h, the resulting suspension was diluted with distilled water and vacuum filtered repeatedly until the pH value of 7 was attained. The sample was then dried in a vacuum oven at 60°C for 12 h. The solid lumps obtained after drying were pounded into a fine powder using mortar and pestle. Acid-treated CNTs are referred as C-CNTs hereafter.

2.2d *Silanation*:

For silane modification of CNTs, acid-treated CNTs (C-CNTs) were dispersed in a solution of ethanol/water (95:5 by volume) consisting of 2% ATPS. The mixture was sonicated and aged with stirring for 4 h. The resulting silanized CNTs were separated by vacuum filtration and washed using acetone and water, dried in a vacuum oven at 60°C for 12 h. Silanized CNTs are referred as S-CNTs.

2.2e *Carbonylation*:

In this process, C-CNTs were suspended in thionyl chloride ($SOCl_2$) and then refluxed for 24 h at 65°C. Then, the suspension was vacuum filtered using a 0.22 μm Millipore PTFE membrane and dried in a vacuum oven for 12 h at 60°C. These CNTs are hereafter referred as T-CNTs.

2.2f *Amination*:

In amination process, T-CNTs were suspended in EDA and refluxed at 60°C for 24 h. Later, the suspension was vacuum filtered using a 0.22 μm Millipore PTFE membrane and dried in a vacuum oven for 12 h at 60°C. Aminated CNTs are hereafter referred as A-CNTs. Figure 1 shows the schematic representation of the functionalization of CNTs.

2.2g *Preparation of POM/MWCNT composites*:

Prior to the preparation of POM/CNT nanocomposites by melt compounding followed by injection moulding, POM and CNTs are dried in a vacuum oven at 60°C for 12 h to ensure the removal of moisture if any. Initially, to assess the effective functionalization among the various methods considered in this, nanocomposites with constant weight fraction (i.e., 0.5 wt%) of various functionalized CNTs were developed. To study the effect of CNT weight fraction, nanocomposites with varying weight fractions of silanized CNTs (0.25, 0.5, 1, 1.5 and 2%) were developed. CNTs were melt-blended with POM using a DTS 25 twin screw extruder with a barrel diameter of 25 mm and L/D of 32. Before melt compounding, the desired quantity of POM and CNTs were pre-mixed thoroughly in a high speed mixer. Then, this mixture was fed through the throat of the extruder. The temperature along the barrel was set between 180 and 190°C and screw speed was set at 100 rpm. The extrudate was obtained in the form of a cylindrical rod and was subsequently cooled in a water bath before cutting into pellets using a pelletizer.

After melt compounding, all the batches were dried overnight in a vacuum oven at 60°C prior to injection moulding. All the batches were injection moulded into dumbbell shaped and flat test bars using a fully automatic vertical screw type injection moulding machine. A moulding pressure of 125 MPa, temperature of 180°C, fill time of 5 s and cooling time of 20 s is maintained during the injection moulding process. Table 1 provides the nomenclature and weight fractions of the constituents of the different nanocomposites.

2.3 *Characterization*

2.3a *Spectral analysis*:

Fourier transform infrared (FTIR) spectra of purified and surface-modified CNTs were recorded to detect new absorption bands if any during chemical modification. For sample preparation, about 2 mg of the CNTs were mixed with KBr and milled thoroughly until a fine mixture is obtained. This mixture was compressed into pellets and then analysed using a Nicolet 6700 FT-IR Spectrometer. The spectra were recorded with a resolution of 2 cm^{-1} in the range of 4000–700 cm^{-1}.

2.3b *Mechanical properties*:

Prior to testing, all samples were conditioned for 48 h at 50% (±5) relative humidity and a temperature of 25°C.

2.3c *Tensile properties*:

Tensile testing was carried out in accordance with ASTM D 638-08 (Type I), a standard test method for determining tensile properties of plastics. A universal testing machine INSTRON 8801 equipped with a 100 kN load cell was used to perform the tensile tests. All the tests were carried out with a gauge length of 50 mm and a cross head speed of 5 mm min^{-1}. The tests were repeated for
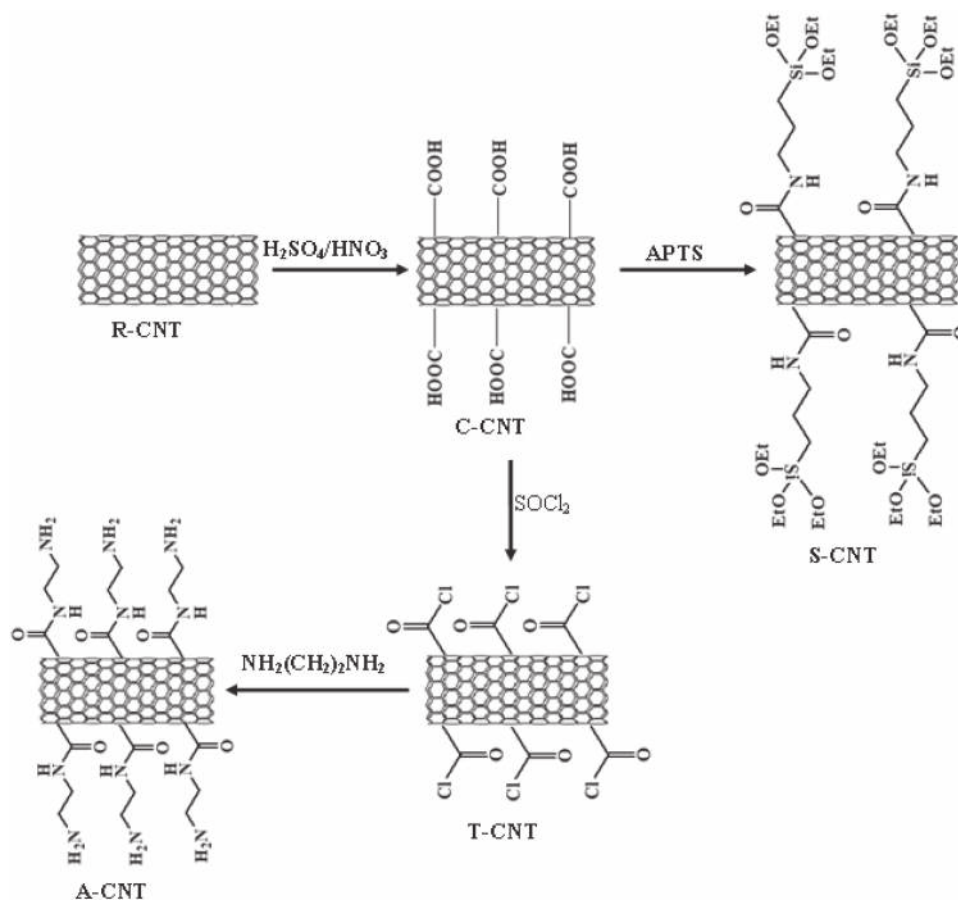
Figure 1. Schematic representation of functionalization of CNTs.

Table 1. Composites identification and constituent composition.

Specimen code	POM (%)	CNTs (%)	Functionalization
A	100	—	—
B	99.5	0.5	Purified
C	99.5	0.5	Carboxylation
D	99.5	0.5	Silanation
E	99.5	0.5	Carbonylation
F	99.5	0.5	Amination
G	99.75	0.25	Silanation
H	99	1	Silanation
I	98.5	1.5	Silanation
J	98	2	Silanation

six samples, and their mean values were reported along with standard deviations.

2.3d Flexural properties: Flexural testing was performed using an INSTRON 8801 universal testing machine in accordance with ASTM D 790 standard. All tests were carried out in 3-point bending mode with a span length of 48 mm and a cross head speed of 2 mm min^{-1}. The tests were repeated for

six samples, and their mean values were reported along with standard deviations.

2.3e Impact testing: Notched Izod impact strength was measured using a Tinius Olsen Impact tester according to ASTM D 256. Specimens having dimensions of 63.5 × 12.7 × 3 mm^3 with a notch angle of 450 and V-notch depth of 2.54 mm were used for carrying out the tests. Ten samples from each category were tested to determine the mean value.

2.3f Fatigue properties: Fatigue tests were performed on composites A, B, D, H and P using Instron 8801 in the tension–tension regime. The fatigue tests were load controlled with a frequency of 5 Hz. The wave form of the cyclic loading is sinusoidal. Tension–tension fatigue testing was conducted at a stress ratio of 0.3 and the maximum applied stress ranged between 20 and 50% of the static strength. These loading levels were selected to ensure that the fatigue life of the studied composites were in the range of low cycle fatigue regimes to high cycle fatigue regimes. Three replicate tests were conducted for each stress level to obtain reliable experimental data.

2.3g *Wear tests*: Dry sliding wear tests were performed on the developed nanocomposites using a pin-on-disc apparatus to study the wear behaviour of the composites. Wear tests were conducted in accordance with ASTM D 3702. Specimens for wear tests having dimensions $3 \times 3 \times 25$ mm^3 were cut from the injection moulded flat test bars. The abrasion area of the sample was 3×3 mm^2. Wear specimen pin is rotated on a flat steel disc of $\sim$10 mm thick and 180 mm in diameter. The initial surface roughness of the steel counterpart was maintained at 0.25 μm for every test. Each specimen was subjected to three different loads (15, 25 and 35 N) and the test was performed at the sliding velocity of 1 m s^{-1} for 30 min. During each test, frictional force was measured and recorded into the computer dynamically. The ratio between the frictional force and load applied gives the coefficient of friction. The specimens and disc were cleaned initially before the beginning of each test to remove the adhered impurities, if any. Mass loss of the specimen was measured before and after the test to measure the specific wear rate by using the following equation:

$$W_s = \Delta m / \rho F_n L \ (\mathrm{mm}^3 \ \mathrm{N}^{-1} \ \mathrm{m}^{-1}), \tag{1}$$

where Δm is the change in weight of the specimen in g, ρ the density of the specimen in g mm^{-3}, F_n the applied load in Newton and L the sliding distance in m. Three repetitive tests were performed for each specimen and average values were reported for friction coefficient and specific wear rate.

2.3h *Morphological studies*: In this work, morphology of tensile fractured surfaces was examined by using a Zeiss EVO 50 Scanning Electron Microscope (SEM). SEM was operated with an acceleration voltage of 10 kV. Prior to SEM observations, all samples were ion-sputter-coated with gold to make them conductive. An Olympus optical microscope with image analyser software is used to analyse the morphology of worn surfaces. TEM images of the composites were carried out using a TECNAI F 30 TEM.

3. Results and discussion

3.1 *Spectral analysis*

Both the raw and functionalized CNTs were characterized by FTIR spectroscopy to confirm the surface modifications of CNTs. FTIR spectra of raw and functionalized CNTs in the region 4000–400 cm^{-1} are presented in figure 2a–e. The peaks observed for acid-treated CNTs (figure 2b) at 3400 cm^{-1} (stretching frequency of –OH) and 1380–1740 cm^{-1} region can be attributed to the C=O stretching vibration of the carboxylic group, which means that –COOH functional groups were generated on the CNT surface after acid treatment [24]. In the case of T-CNTs (figure 2c), a sharp peak at 610 cm^{-1} corresponds to the C–Cl bond stretching vibration, indicating the formation of a OH–C–Cl moiety during the treatment of
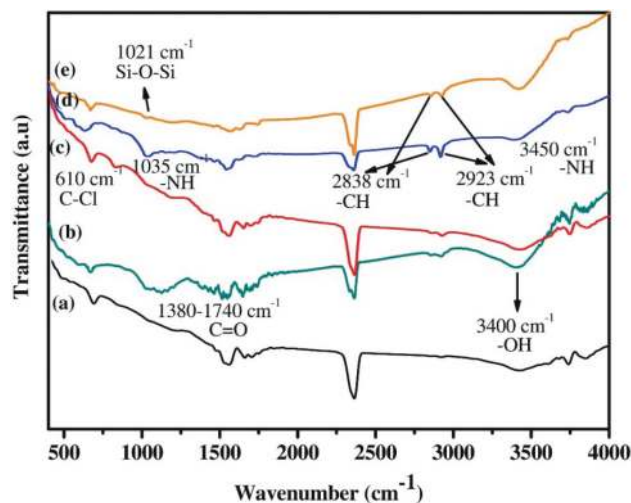

Figure 2. FTIR spectra of (**a**) raw CNTs, (**b**) C-CNTs, (**c**) T-CNTs, (**d**) A-CNTs and (**e**) S-CNTs.

acid-treated CNTs with thionyl chloride (SOCl$_2$). The spectra of aminated CNTs (figure 2d) reveal that the peaks at 2838 and 2923 cm^{-1} correspond to stretching vibration of –CH bond. Furthermore, small humps observed at 1035 and 3450 cm^{-1} may be attributed to –NH bonds, which arise because of CNTs reaction with EDA. From the spectra of silane functionalized CNTs (figure 2e), a peak can be observed at 1021 cm^{-1}, which can be attributed to asymmetric stretching vibration of Si–O–Si bonds due to formation of silaxone units during silanization of CNTs [25].

3.2 *Tensile and flexural properties*

The effect of CNT functionalization on tensile strength and modulus of POM/CNT nanocomposites is shown in figure 3. Reinforcing POM with 0.5 wt% of raw CNTs resulted in a slight decrease of tensile strength by 2.8% and marginal improvement of stiffness by 9% as compared to neat POM. In sharp contrast, reinforcing effect of CNTs is clearly apparent in the case of surface-modified CNTs. Tensile strength and stiffness were found to be improved by incorporation of C-CNTs, S-CNTs, T-CNTs and A-CNTs. Among various surface modifications, silanization of CNTs (composite D) resulted in maximum improvement of tensile strength and modulus by $\sim$23 and 38%, respectively.

As evident from the SEM images (figure 4b–e), improved compatibility between CNTs and matrix as compared to raw CNTs might have resulted in improvement of tensile properties. In the case of composites with C-CNTs (figure 4b), T-CNTs (figure 4d) and A-CNTs (figure 4e), a few pullouts were present indicating moderate adhesion between CNTs and POM. Whereas in the case of composites with silanized CNTs, pullouts are hardly seen indicating a strong interaction between CNTs and POM.
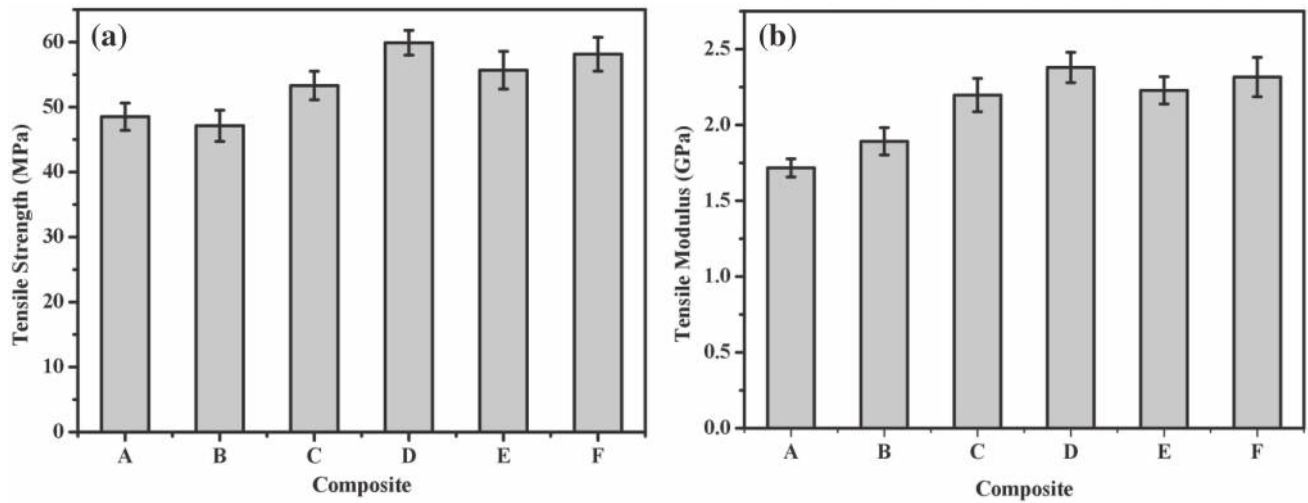
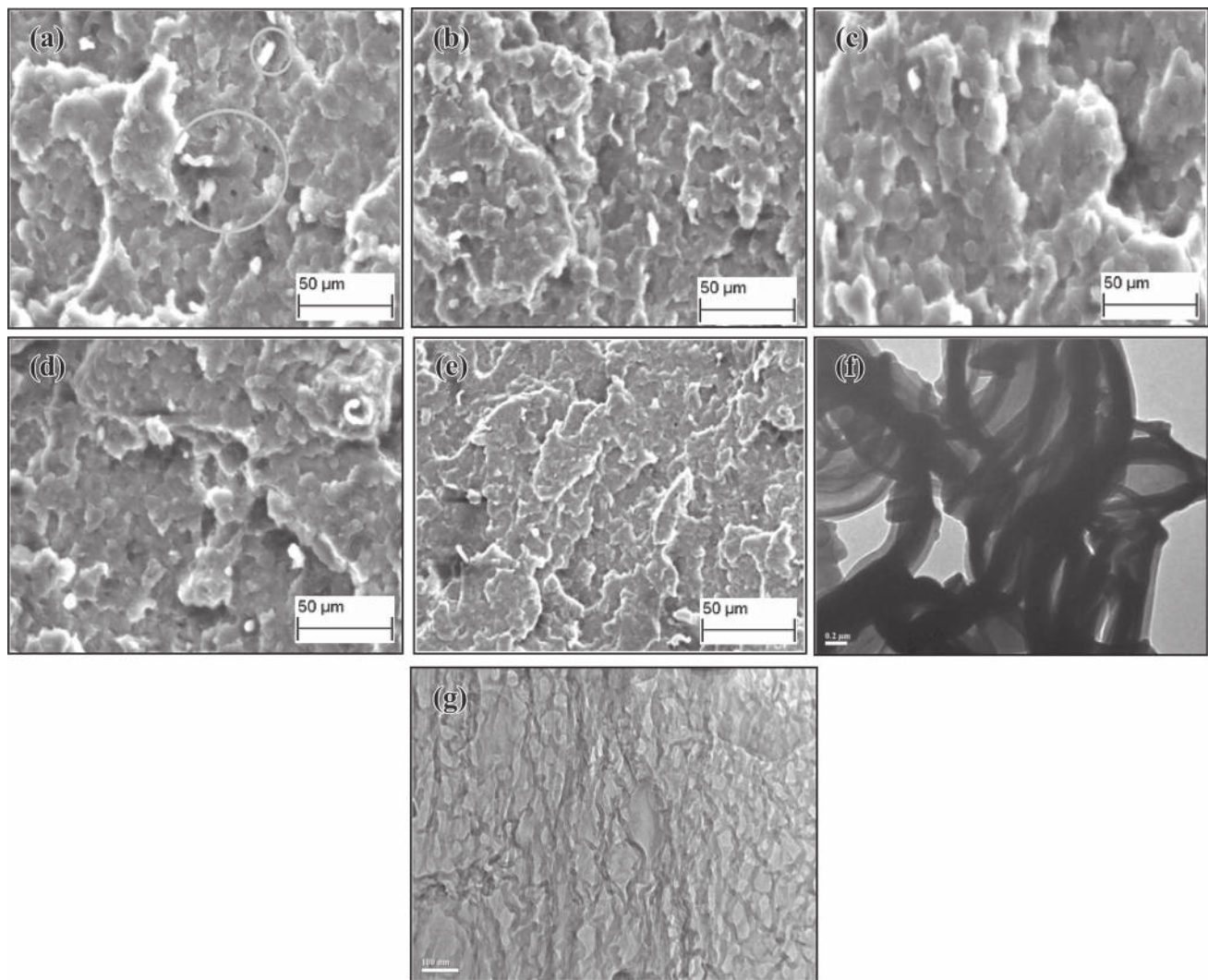**Figure 3.** Effect of CNT functionalization on (**a**) tensile strength and (**b**) tensile modulus.

Figure 4. SEM images of tensile fractured surfaces of composites: (**a**) A (POM only), (**b**) B (POM + raw CNT), (**c**) C (POM + C-CNT), (**d**) D (POM + S-CNT), (**e**) E (POM + T-CNT) and TEM images of composites: (**f**) B (POM + raw CNT) and (**f**) D (POM + S-CNT).
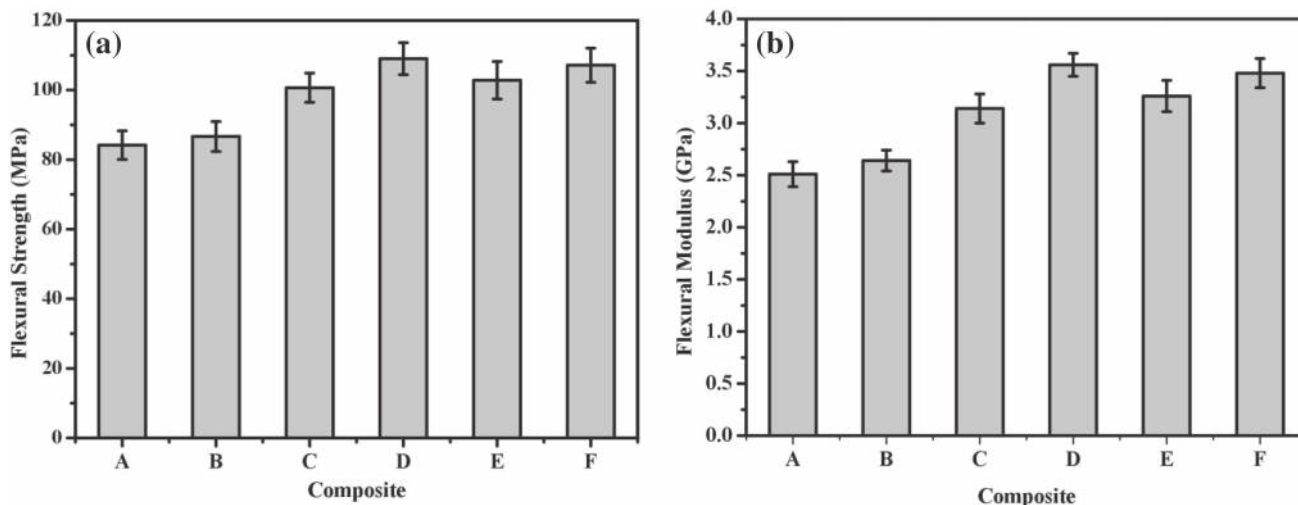
Figure 5. Effect of CNT functionalization on (**a**) flexural strength and (**b**) flexural modulus.
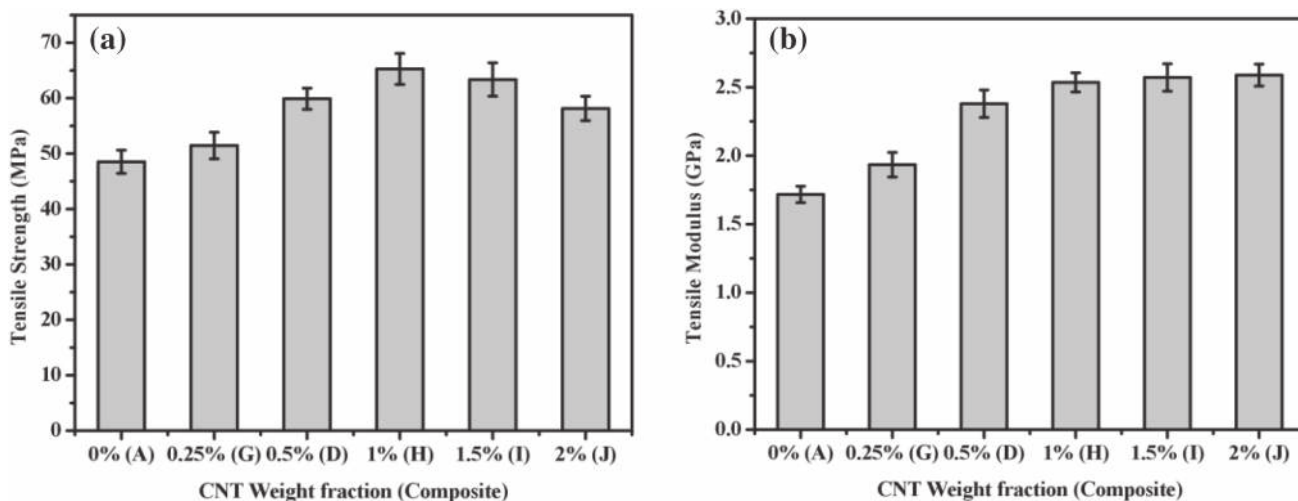

Figure 6. Variation of (**a**) tensile strength and (**b**) tensile modulus with CNT content.

A decrease in the strength of composite B as compared to POM may be attributed to poor dispersion of raw CNTs in the POM matrix and low interfacial bond strength between CNTs and matrix. Significant improvement of tensile properties of POM with incorporation of functionalized CNTs might be attributed to uniform dispersion of CNTs in matrix and improved interfacial adhesion between CNTs and matrix. TEM images of composites B and D are shown in figure 4. As seen from figure 4f, raw CNTs (composite B) resulted in a densely entangled network indicating non-uniform dispersion, while silanized CNTs are uniformly dispersed as shown in figure 4g. Lee *et al* [26] reported a similar result, where silane modification of CNTs resulted in increase of interfacial strength between CNTs and matrix.

To quantitatively determine interfacial adhesion and interfacial shear strength for composites B, C, D, E and F, they are evaluated by using Pukanszky model based on classical Kelly–Tyson equation [27,28]:

$$A = (\sigma_m (B - 2.04))/\eta\alpha, \tag{2}$$

where $B = \ln[\sigma_r(1 + 1.25\varphi_f)/1 - \varphi_f]/\varphi_f$ and τ is interfacial shear strength, σ_m is tensile strength of matrix, σ_r is relative strength as σ_c/σ_m where σ_c is tensile strength of nanocomposite, η is an orientation factor, α is aspect ratio of CNT as ratio of length to diameter of CNT and φ_f is the volume fraction of CNTs. The computed interfacial shear strengths for composites B, C, D, E and F are -1.81, 6.49, 15.69, 9.69 and 12.75 MPa, respectively. The negative interfacial shear strength for composite B indicates that the reinforcing effect of raw CNT is zero. Among various types of functionalizations, silanized CNTs exhibited the maximum
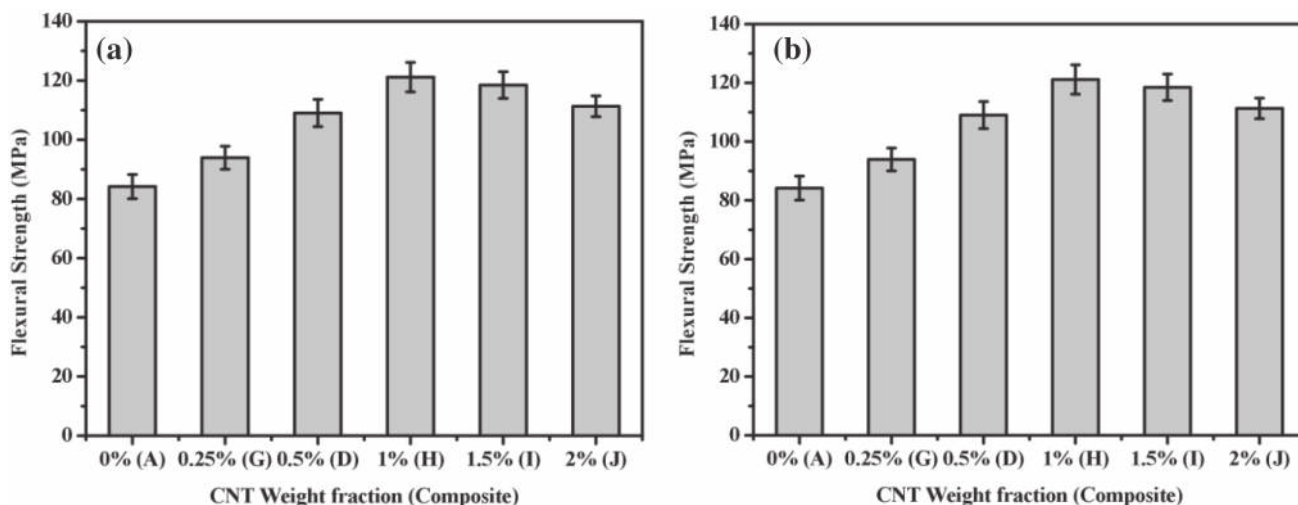
Figure 7. Variation of (**a**) flexural strength and (**b**) flexural modulus with CNT content.

interfacial shear strength indicating the effective transfer of applied load from matrix to silanized CNTs by means of shear forces at the interface. Thus, the enhanced interfacial adhesion and uniform dispersion of silanized CNTs in the matrix might have been the major reasons for improvement of tensile properties of composite D.

The effect of functionalization of CNTs on flexural strength and modulus is shown in figure 5. Unlike tensile strength, flexural strength marginally improved by 3% in the case of raw CNTs as compared to neat POM. Functionalization of CNTs resulted in improvement of flexural properties. Composites with silanized CNTs exhibited maximum improvement of flexural strength and modulus by 29 and 34%, respectively.

The effect of CNT content on tensile and flexural properties of the nanocomposites is shown in figures 6 and 7, respectively. From figures 6 and 7, it can be seen that the tensile and flexural strengths increased with an increase in CNT content up to 1 wt%. Beyond 1 wt% CNTs, a decline in tensile and flexural strengths was observed. In contrast to tensile strength, tensile and flexural moduli of the composites increased with the increase in CNT content. However, beyond 1 wt% CNTs improvement in modulus is marginal. Whereas for the composites with < 1 wt% CNT content (i.e., composites D, G, H) significant enhancement of modulus is observed with the increase in CNT content. Decline in tensile and flexural strengths beyond 1 wt% CNTs may be attributed to non-homogeneous dispersion and aggregation of CNTs inside the composite. Overall, incorporation of 1 wt% silanized CNTs in POM resulted in the enhancement of tensile strength, tensile modulus, flexural strength and flexural modulus by ~34, 46, 43 and 48%, respectively.

3.3 *Impact toughness*

The effect of functionalization and weight fraction of CNTs on the impact toughness is presented in figures 8 and 9,

respectively. As seen from figure 8, the addition of raw CNTs in POM decreased impact toughness by ∼ 2%, whereas nanocomposites C, D, E and F with functionalized CNTs exhibited a moderate increase in impact toughness by 6, 12, 7 and 11% respectively. In the case of composites with raw CNTs, decrease in impact toughness may be due to weak interfacial interaction between CNTs and matrix. Due to the weak interfacial interaction, cracks propagate at a faster rate and thereby results in lower impact toughness as compared to neat polymer. In the case of composites with functionalized CNTs, relatively strong interfacial interaction between matrix and CNTs offers a torturous path to the propagation of cracks and thereby resulted in enhancement of impact toughness [29]. Many studies have demonstrated that that the improved impact strength of functionalized CNT composites is due to the enhanced interfacial bond strength between CNT and matrix [30–33]. The strong interfacial adhesion promotes crack bridging phenomenon and local plastic deformation
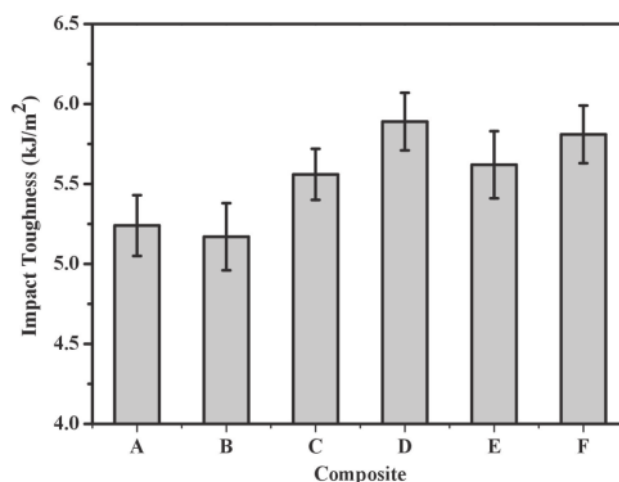

Figure 8. Effect of CNT functionalization on impact toughness.

of matrix which in turn offers more torturous path to crack propagation. A higher strain to failure ratio of CNTs allows the CNTs to bridge the range of crack openings and thereby results in absorbing the fracture energy. If interfacial bond

Figure 9. Variation of impact toughness with CNT content.

strength is weak, effective crack bridging cannot occur, there by resulting in faster crack propagation and lower impact strength. Chandrasekharan *et al* [32] reported that in Epoxy graphene composites, the crack path gets deflected whenever the crack tip meets the graphene sheet, thereby causing the crack to take a torturous path. Wang *et al* [33] observed a substantial enhancement of impact strength of by incorporating functionalized CNTs. The authors attributed the enhancement of impact strength to good CNT matrix adhesion that allows effective load transfer at CNTs crack bridging.

Among the various types of functionalization considered in this work, composite D (S-CNTs) exhibited maximum improvement in toughness by ~12%. As seen from figure 10, impact toughness increased with an increase in silanized CNT content up to 0.5 wt%. However, beyond 0.5 wt%, impact toughness becomes more or less saturated, indicating that higher content CNTs would not result in any further increase in impact toughness as there is a chance for increasing of agglomerations with increasing CNT content. Significant enhancement of tensile properties is achieved in this work by incorporating 1 wt% silanized CNTs as compared to some of the already existing reports [18,34–37] that are presented in table 2.
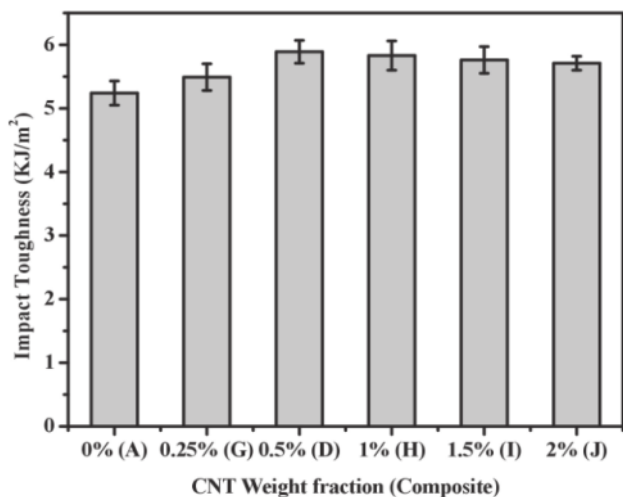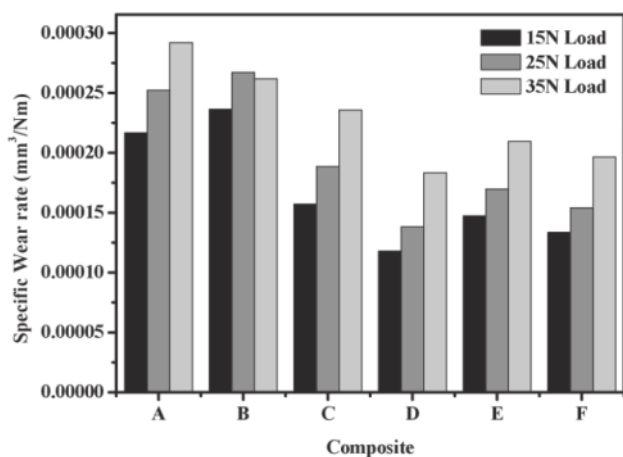

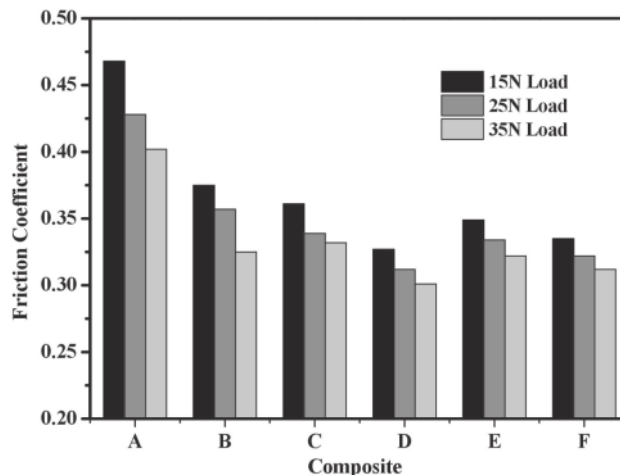**Figure 10.** Effect of CNT functionalization on specific wear rate.

Figure 11. Effect of CNT functionalization on friction coefficient.

Table 2. Comparison study of mechanical properties with the existing work.

| Matrix | Functionalization | Weight fraction (%) | % increase in tensile properties | | Reference |
			Tensile strength	Tensile modulus	
PI	Acid treatment	7.0	19	39	[34]
Epoxy	Silane treatment	0.25	3.6	8.7	[35]
PP	Silane treatment	1	55	—	[36]
PVC	Silane treatment	1	26	—	[36]
Epoxy	Silane treatment	1	50	—	[36]
PA	Di-amine treatment	1	−5.3	6.1	[18]
PE	Amine treatment	1.5	−17	22	[37]
POM	Silane	1	34	46	Present study
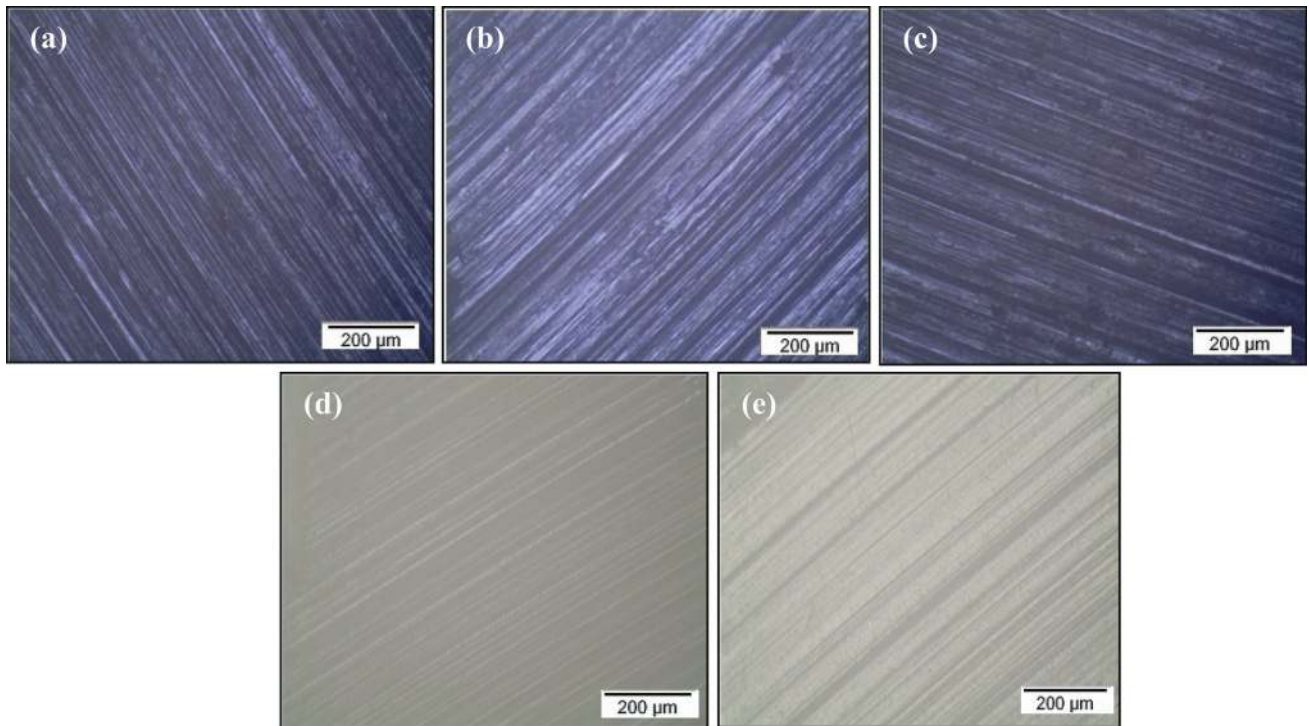
Figure 12. Worn surfaces of (**a**) POM at 15 N load, (**b**) POM at 35 N load, (**c**) composite B, (**d**) composite D and (**e**) composite H.
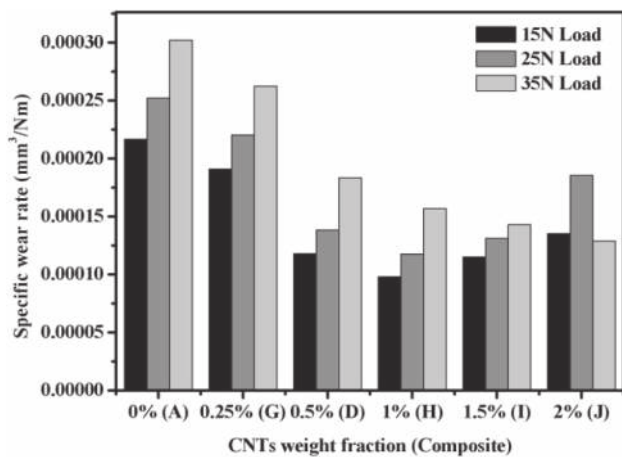

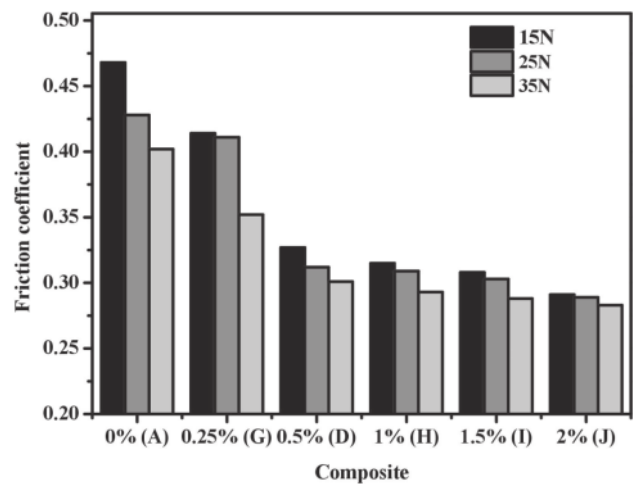**Figure 13.** Variation of specific wear rate with CNT content.

Figure 14. Variation of friction coefficient with CNT content.

3.4 *Wear*

Dry sliding wear tests were conducted on the developed composites at three different loads. The effect of CNT functionalization on the specific wear rate and coefficient of friction is presented in figures 10 and 11, respectively. From these figures, an increase in specific wear rate and decrease in coefficient of friction can be observed with the increase in applied load. Worn surfaces of POM at 15 and 35 N loads are shown in figure 12a and b, respectively. Deep groves formed at 35 N load (figure 12b) as compared to shallow groves formed

at 15 N load (figure 12a) indicate the influence of load on the wear of the composites. Enhanced specific wear rate at higher loads may be attributed to increased real contact area between the composite and counter surfaces [38]. As seen from figure 10, an increase in specific wear rate by ∼9 and 6% can be observed at 15 and 25 N loads respectively, for composite B (0.5 wt% R-CNTs), while at a higher load i.e., at 35 N, the specific wear rate decreased by ∼13% with the addition of R-CNTs. The less wear resistivity of composite B with the addition of raw CNTs may be attributed to

weak interfacial strength between CNTs and POM. Under low applied loads, aggregates of pulled out CNTs will act as third body material and causes severe wear, contributing to a significant increase in the wear rate of the specimens. However, under higher loads, aggregates crush into smaller ones, which will not have a severe abrasive effect and thereby results in enhancement of wear resistance. Among the types of functionalizations considered in this work, the composite with S-CNTs exhibited a higher wear resistance and the lowest coefficient of friction at all the applied loads. Improved interfacial adhesion by incorporation of silanized CNTs might have resulted in decrease of stress concentration and increase in wear resistance. Moreover, strength, stiffness and toughness

of the material significantly influence the wear behaviour of the material [39]. Thereby, improved strength, toughness and stiffness by incorporation of silanized CNTs might also have contributed to the significant improvement of wear resistance. The smooth worn surface of composite D (S-CNTs) (figure 12d) as compared to POM (figure 12a) and composite B (R-CNTs) (figure 12c) indicates better wear resistance.

The effect of CNT content on the wear rate and coefficient of friction is presented in figures 13 and 14, respectively. Wear rates decreased with increase in CNT content up to 1 wt% at all the applied loads. Beyond 1 wt% CNT content, the wear rate increased with increase in CNT content. Decrease in wear resistance at higher CNT content might be ascribable to the abrasive action of CNT aggregates. As seen from figure 14, friction coefficient decreased with increase in CNT content. From the worn surface of composite H (figure 12e), less number of shallow groves can be observed as compared to composite D (figure 12d), indicating the effect of CNT content on the improvement of wear resistance.

3.5 *Fatigue behaviour*

To assess the effect of CNT functionalization and content on fatigue behaviour, tension–tension fatigue tests were carried out on composites A (POM), B (0.5 wt% R-CNT), D (0.5 wt% S-CNTs) and H (1 wt% S-CNTs). Table 3 lists the experimental results of the fatigue tests. Figure 15 shows the relationship between the maximum applied stress and fatigue lives of the studied composites. Fatigue life data were fitted using power law model [40]:
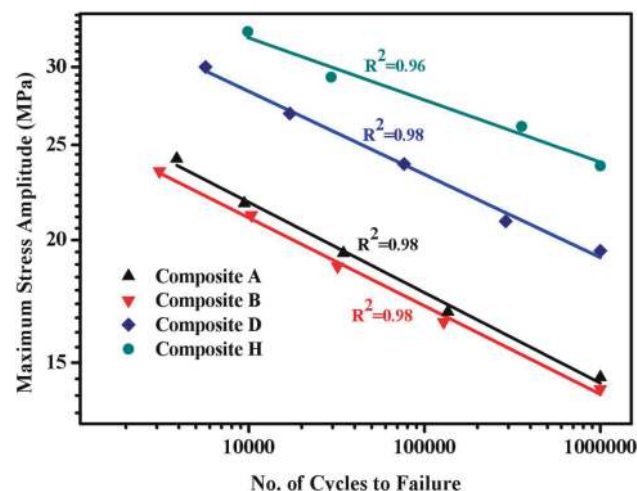
Figure 15. Fatigue lives of the composites.

$$\sigma_{\max} = ANf^{B}, \tag{3}$$

Table 3. Experimental results of the fatigue tests.

Composite	Static strength (MPa)	Stress amplitude level (%)	Maximum stress (MPa)	Mean cycles to failure (N_f)	Fatigue strength coefficient, A	Fatigue strength exponent, B
A	48.5	50	24.2	3891	51.003	−0.092
		45	21.8	9437		
		40	19.4	34,589		
		35	16.9	135,677		
		30	14.5	1,000,000		
B	47.1	50	23.5	3103	48.190	−0.089
		45	21.2	10,349		
		40	18.8	31,993		
		35	16.5	128,573		
		30	14.1	1,000,000		
D	59.9	50	30	5675	61.74	−0.084
		45	26.9	17,118		
		40	23.9	76,457		
		35	20.9	289,421		
		32.5	19.5	1,000,000		
H	65.3	50	32.6	9876	57.505	−0.063
		45	29.3	29,419		
		40	26.1	356,391		
		35	22.8	1,000,000		

where *A* is a fatigue strength coefficient and *B* is fatigue strength exponent. The constants *A* and *B* are given in table 3 and the fitted curves are plotted in figure 15. As seen from figure 15, addition of 0.5 wt% raw CNTs resulted in decrease of fatigue strength. The decrease in fatigue strength with the addition of raw CNTs may be due to the weak interaction between the CNTs and matrix. The effect of CNT functionalization and content on fatigue strength can be observed from the S–N curves of composites D and H. Functionalization of CNTs has resulted in significant improvement in fatigue strength as compared to neat POM and nanocomposites with raw CNTs. Similarly, composite with 1 wt% S-CNTs exhibited more fatigue strength than the composite with 0.5 wt% S-CNTs. This enhancement might be attributed to strong interfacial bonding between CNTs and matrix.

4. Conclusion

In the present study, tensile, flexural, impact, wear and fatigue behaviour of POM/CNT nanocomposites were studied as a function of CNT functionalization and concentration. FTIR spectroscopic studies revealed that all the functionalization methods used in this study resulted in the modification of CNT surface. As compared to raw CNTs, functionalized CNTs resulted in improvement of strength, modulus and impact toughness of the composites. Among various types of functionalizations, silanized CNTs had higher reinforcing efficiency for POM, which could be ascribed to better dispersion of S-CNTs and stronger interfacial bonding between S-CNTs and POM matrix. Furthermore, it was also found that functionalization and concentration of CNTs have profound influence on wear and fatigue behaviour of composites. Nanocomposites with 1 wt% of S-CNTs resulted in maximum improvement of wear resistance and fatigue life.

Acknowledgements

References

[1] Imrek H 2009 *Tribol. Int.* **42** 503
[2] Duzcukoglu H 2009 *Tribol. Int.* **42** 1146
[3] Ijima S 1991 *Nature* **354** 56
[4] Dresselhaus M S, Dresselhaus G and Saito R 1995 *Carbon* **33** 883
[5] Fiedeler B and Gojny F H 2006 *Compos. Sci. Technol.* **66** 3115
[6] Ma P-C, Siddique N A, Marom G and Kim J K 2010 *Composites, Part A* **41** 1345
[7] Yousef S, Visco A M, Galtieri G and Njuguna J 2016 *J. Miner. Metals Mater. Soc.* **68** 288
[8] Zeng Y, Ying Z, Du J and Cheng H M 2007 *J. Phys. Chem. C* **111** 13945
[9] Zhao X and Ye L 2010 *J. Polym. Sci. B: Polym. Phys.* **48** 905. https://doi.org/10.1002/polb.21977
[10] Wang F, Wu J K, Xia H S and Wang Q 2007 *Plast. Rubber Compos.* **36** 297
[11] Jiang Z, Chen Y and Liu Z 2014 *J. Polym. Res.* **21** 451
[12] Kwon J Y and Kim H D 2005 *J. Appl. Polym. Sci.* **96** 595
[13] Hong S-K, Kim D, Lee S, Kim B W, Theilmann P and Park S H 2015 *Composites, Part A* **77** 142
[14] Zhao C, Hu G, Justice R, Schaefer D W, Zhang S, Yang M *et al* 2005 *Polymer* **46** 5125
[15] Kim M-G, Moon J-B and Kim C-G 2012 *Composites, Part A* **43** 1620
[16] Ma P C, Kim J-K and Tang B Z 2007 *Compos. Sci. Technol.* **67** 2965
[17] Liu T, Tong Y and Zhang W-D 2007 *Compos. Sci. Technol.* **67** 406
[18] Meng H, Sui G X, Fang P F and Yang R 2008 *Polymer* **49** 610
[19] Yuen S-M, Ma Chen-Cchi M, Lin Yao Y and Kuan H-C 2007 *Compos. Sci. Technol.* **67** 2564
[20] Cui L-J, Geng H-Z, Wang W-Y, Chen L-T and Gao J 2013 *Carbon* **54** 277
[21] Sulong A B, Park J, Lee N and Goak J 2006 *J. Compos. Mater.* **40** 1947
[22] Lee J-H, Kathi J, Rhee K Y and Lee J H 2010 *Polym. Eng. Sci.* **50** 1433
[23] Zhang W, Picu R C and Koratkar N 2008 *Nanotechnology* **19** 285709
[24] Kuznetsova A, Mawhinney D B, Naumenko V, Yates J T, Liu J and Smalley R E 2000 *Chem. Phys. Lett.* **321** 292
[25] Satyanarayana N, Xie X and Rambabu B 2000 *Mater. Sci. Eng. B* **72** 7
[26] Lee J-H, Rhee K Y and Park S J 2011 *Composites, Part A* **42** 478
[27] Lazzeri A and Phuong V U 2014 *Compos. Sci. Technol.* **93** 106
[28] Zare Y 2015 *Mech. Mater.* **85** 1
[29] Saha S and Bal S 2017 *Bull. Mater. Sci.* **40** 945
[30] Saminathan K, Selvakumar P and Bhatnagar N 2008 *Polym. Test.* **27** 453
[31] Ghoshal S, Wang P H, Gulgunje P, Verghese N and Kumar S 2016 *Polymer* **100** 259
[32] Chandrasekaran S, Sato N, Tolle F, Mülhaupt R, Fiedler B and Schulte K 2014 *Compos. Sci. Technol.* **97** 90
[33] Wang P H, Sarkar S, Gulgunje P, Verghese N and Kumar S 2018 *Polymer* **151** 287
[34] Yuen S M, Ma C C M, Lin Y Y and Kuan H C 2007 *Compos. Sci. Technol.* **67** 2564
[35] Geng Y, Liu M Y, Li J, Shi X M and Kim J K 2008 *Composites, Part A* **39** 1876
[36] Mashhadzadeha A H, Fereidoona A B and Ahangari M G 2017 *Appl. Surf. Sci.* **420** 167
[37] Yang B X, Pramoda K P, Xu G Q and Goh S H 2007 *Adv. Funct. Mater.* **17** 2062
[38] Chang B-P, Md Akil H, Md. Nasir R B 2013 *Wear* **297** 1120
[39] Chand N and Dwivedi U K 2006 *Wear* **261** 1057
[40] Hwang W and Han K S 1986 *J. Comp. Mater.* **20** 154